Supplemental Figures and Legends

FIG S1_Munding (Ares)

Figure S1. Related to Figure 3. Rapamycin-induced improvement in splicing.

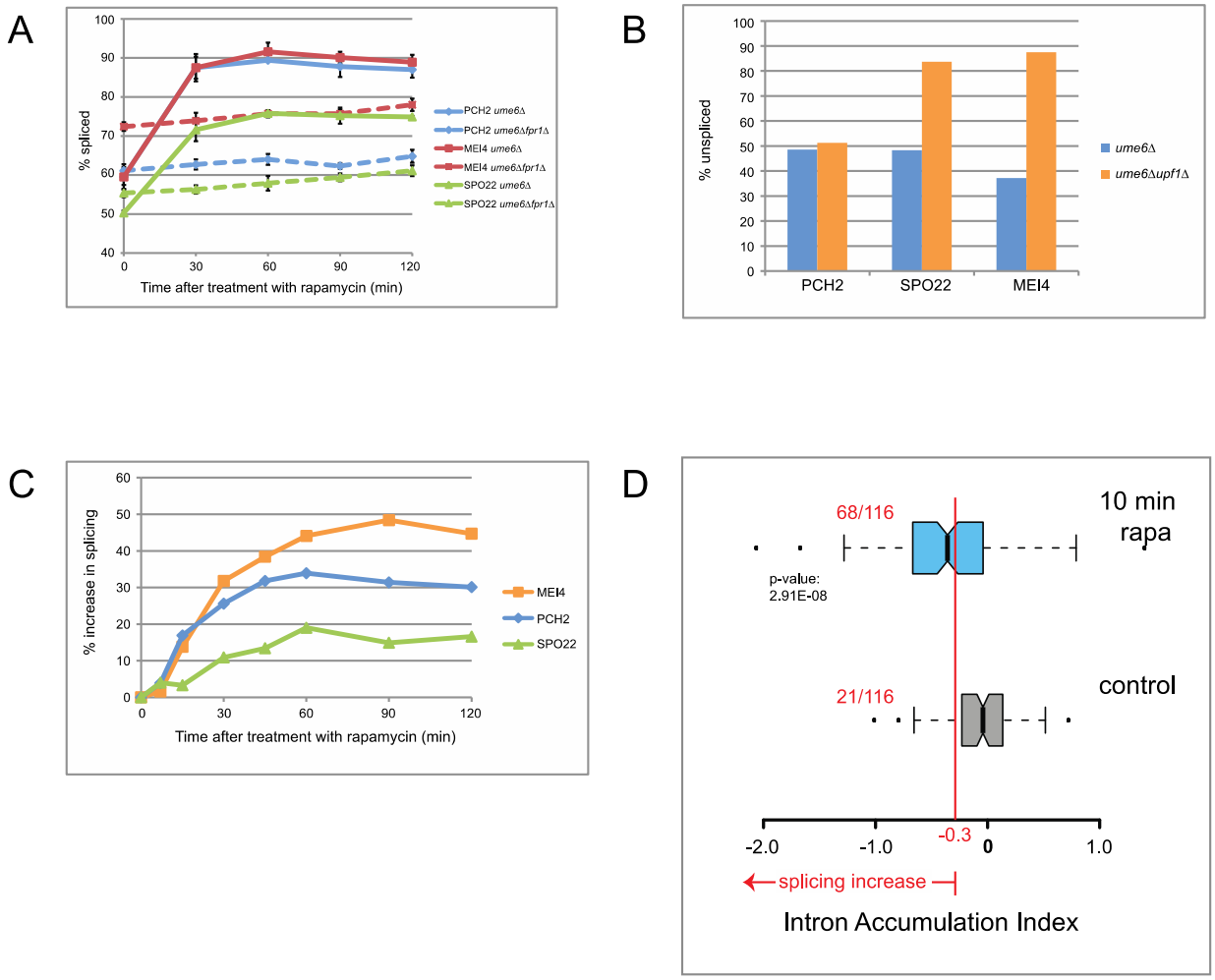

Figure S1. Related to Figure 3. Rapamycin-induced improvement in splicing. (A) Quantification of splicing efficiency of meiotic transcripts *SPO22*, *MEI4* and *PCH2* by semi-quantitative RT-PCR in *ume6*Δ and *ume6*Δ*fpr1*Δ vegetative cells at indicated times after

treatment with rapamycin. The *FPR1* gene encodes the cofactor required for rapamycin binding to TOR. Error bars represent ± 1SD. (B) Quantification of unspliced pre-mRNA of *SPO22*, *MEI4* and *PCH2* by semi-quantitative RT-PCR in *ume6*Δ and *ume6*Δ*upf1*Δ vegetative cells. *SPO22* and *MEI4* are substrates of NMD while *PCH2* is a poor NMD substrate. (C) Quantification of percent increase in splicing of *SPO22*, *MEI4*, and *PCH2* by semi-quantitative RT-PCR in *ume6*Δ*upf1*Δ vegetative cells at indicated time after treatment with rapamycin. (D) IAI distributions from the average of both biological replicates at 10 minutes after rapamycin treatment relative to untreated samples (also shown in Fig 3D) and control distribution of self comparisons between biological replicates after rapamycin treatment. A t-test indicates these distributions differ significantly, reflecting a change in splicing efficiency. Red line mark 25% splicing improvement (IAI < -0.3) and numbers in red indicate the number of events in each distribution with an IAI < -0.3.

FIG S2_Munding (Ares)

Figure S2. Related to Figure 6. Competitive inhibition.

A

$$V_0 = \frac{V_{max}[S_1]}{Km_{(S_1)} + [S_1] + Km_{(S_1)}\frac{[S_2]}{Km_{(S_2)}}}$$

B

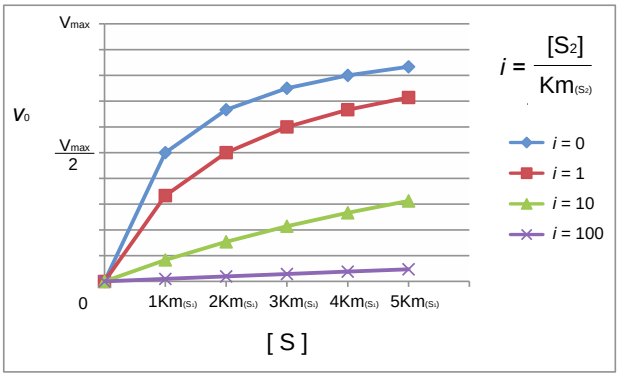

Figure S2. Related to Figure 6. Competitive inhibition. (A) Michaelis-Menten equation for competitive inhibition where the initial velocity (v_0) of the substrate (S_1) is given by presented formula and competing substrate (S_2) acts as the inhibitor. (B) Plot of the initial velocity (V_0) of the substrate (S_1) in the presence of competitor substrate (S_2) that behaves as a competitive inhibitor. *i* is the inhibitory effect of the competitor represented by $\frac{[S_2]}{Km_{(S_2)}}$.

Supplemental Tables

Table S1 (related to Figure 1): Data for heatmap in Figure 1A.

(Excel file)

Table S2 (related to Figure 1, 3, 4): Expression of spliceosomal components during meiosis, rapamycin treatment, and *IFH1* down-regulation.

(Excel file)

Table S3. Yeast Strains.

STRAIN	GENOTYPE	SOURCE NOTES
SK1-K8409	*MATa/MATalpha HO/HO URA3-tetR-GFP/URA3-tetR-GFP URA3:tetO224/URA3:tetO224 REC8-HA3/REC8-HA3 his3::hisG/his3::hisG trp1 /trp1*	ATCC
BY4741	*MATa his3Δ1 leu2Δ0 met15Δ0 ura3Δ0*	Open Biosystems
EMY1	*MATalpha ume6::KANMX6 his3Δ1 leu2Δ0 lys2Δ0 ura3Δ0*	Spore from heterozygous diploid knockout collection; Open Biosystems
EMY2	*BY4741, k-HIS3:GAL1-IFH1*	Integration
SRY4-1b	*MATalpha prp4-1 ade2- leu2-3,112 ura3-52 his3-Δ200*	S. Ruby
EMY3	*prp4-1, k-HIS3:GAL1-IFH1*	spore from EMY2 X SRY4-1b
SRY11-1d	*MATalpha prp11-1 ade2- his- his4- leu2- tyr1- ura3-52*	S. Ruby
EMY4	*prp11-1, k-HIS3:GAL1-IFH1*	spore from EMY2 X SRY11-1d

Table S4. RT-PCR and RT-qPCR primers.

PRIMER NAME	SEQUENCE
qPCR MEI4-inF	5' acgtgaaattgtcacatcctt 3'
qPCR MEI4-exF	5' ccaggaatcctacgttgtgg 3'
qPCR MEI4-exR	5' aggcgcaacccatttgtat 3'
qPCR DMC1-inF	5' gaggttctttccccctttctt 3'
qPCR DMC1-exF	5' gttttgtcaacaacaagaagacat 3'
qPCR DMC1-exR	5' tgataaggagtacacacgctgtc 3'
qPCR SEC14-inF	5' agttctgtctatatgaagcaaaaatga 3'
qPCR SEC14-exF	5' agaaaaggaatttttagaatcctaccc 3'
qPCR SEC14-exR	5' gttcaatgaaaccagcgtctt 3'
qPCR CPT1-inF	5' tgcaccctaaatcttctgtgg 3'
qPCR CPT1-exF	5' tgatgaccgctctttccttt 3'
qPCR CPT1-exR	5' ctggtcaaaatacgggtcgt 3'
qPCR HNT1-inF	5' cacaccaatgatggcgatag 3'
qPCR HNT1-exF	5' gcgaaattccatccttcaaa 3'
qPCR HNT1-exR	5' ggcatagcatcggtaaggaa 3'
qPCR MOB2-inF	5' tctggacctgcgttatcattt 3'
qPCR MOB2-exF	5' aaaaccagcccttaatgttg 3'
qPCR MOB2-exR	5' cggggaaacttgtttgagaa 3'
qPCR RPL34B-inF	5’ gaagtgattactaacattaatgggaaa 3’
qPCR RPL34A/B-exF	5' aggttgttaagaccccaggtg 3'
qPCR RPL34A/B-exR	5' gaaccaccgtaagctctgga 3'
qPCR RPS16A-exF	5' cgatgaacaatccaagaacg 3'
qPCR RPS16A-exR	5' tctggaacgagcacccttac 3'
qPCR RPL28-exF	5' ggtggtcaacatcaccacag 3'
qPCR RPL28-exR	5' ggcttccagaaatgagcttg 3'
qPCR RPS5-F	5' actgaccaaaacccaatcca 3'
qPCR RPS5-R	5’ ttgacgtctagcagcaccac 3’
qPCR RPL11A/B-F	5’ cagaggtccaaaggctgaag 3’
qPCR RPL11A/B-R	5’ taccgaaaccgaagttaccg 3’
qPCR IFH1-F	5’ ttctggtaaactgccagcaaa 3’
qPCR IFH1-R	5’ ggctaaatcttcttggcctcg 3’
qPCR SEC65-F	5' catatggccctgatttcgac 3'
qPCR SEC65-R	5' ggcttgaacgacttttctgc 3'
SPO22-F1	5' tcagaccacaacgttaactc 3'
SPO22-R1	5' tccatagacttgatgctgca 3'
MEI4-F1	5' gaggcaaactggaagatatg 3'
MEI4-R1	5' agagcacctacatcttcgac 3'
PCH2-F1	5' caagatcaactggagtcaag 3'
PCH2-R1	5' tcgtctacaggaaatgtccg 3'

Supplemental Experimental Procedures

Transcriptome Profiling

The microarray data in Fig1 is from four independent meiotic time courses where each meiotic time point was compared to a reference pool RNA comprised of 50% time zero RNA plus 10% each of time 2 hours, 5, hours, 7 hours, 9 hours and 11 hours was used as an arbitrary reference pool (Munding et al., 2010). To evaluate splicing changes the Intron Accumulation Index (IAI) (IAI= $\log_2$ ratio of intron probe - $\log_2$ ratio of exon2 probe) (Clark et al., 2002) was calculated for each intron/time point. The t=0 IAI was then subtracted from each time point IAI to give the change in IAI.

To estimate the magnitude of a change in IAI that would constitute a true splicing change we developed a control distribution of IAIs as a background model that would capture noise in the IAI measurement. To do this we compared IAIs derived from biological replicate samples that should show no change in IAI. We calculated the apparent change in IAI for each of the 156 genes by comparing the two samples from 2 hours of meiosis, the two from 5 hours and the two from 7 hours and averaged these IAIs to create the control distribution. We determined that only 10 of 156 genes showed a change in IAI of >40% (1.4 fold) in the control distribution, suggesting that this threshold is associated with an FDR of less than 0.1.

To generate the image in Fig 1A, we used Gene Cluster 3.0 (de Hoon et al., 2004) and Java Treeview (Saldanha, 2004). The pie chart in Fig1C includes 156 intron-containing genes whose expression does not decrease more than 2-fold (Log_2 Ratio ≥ -1.0) during the meiotic time course. Introns with a zero-subtracted IAI < -0.5 (indicating at least a 40% improvement in splicing) at two out of three mid-meiotic time points (t=2, 5, 7h after induction of meiosis) are called as “increased splicing”; similarly introns with a zero-subtracted IAI ≥ 0.5 at two out of

three mid-meiotic time points are called “decreased splicing”, while no change in splicing is signified by 0.5 > IAI > -0.5.

The data described in Fig 3 and Fig 4 was collected using RNA-Seq. RNA from the respective strains was isolated and DNased using Turbo DNase (Life Technologies) and RNA quality was assayed using the 2100 Bioanalyzer (Agilent). Poly(A) RNA was selected from 20µg total RNA using oligo-(dT) Dynabeads (Life Technologies). Strand-specific cDNA sequencing libraries were prepared as described in (Yassour et al., 2010) and paired-end sequenced on the HiSeq2000 (Illumina). Reads were mapped using TopHat (Trapnell et al., 2009) which aligns reads using Bowtie2 (Langmead and Salzberg, 2012). Changes in gene expression were estimated by comparing the $\log_2$ ratios of the exon 2 reads. Splicing changes were estimated by calculating an IAI using counts of intron-containing reads relative to exon 2 reads in treated samples relative to control. To produce the box plots in 3C, intron-containing events with junction reads and at least 50 exon 2 reads were used. To produce the histogram in Fig 3D, only introns with splice junction reads and at least 50 exon 2 reads whose gene expression did not change by 2-fold or greater were used. The IAIs of the biological replicates were averaged. To produce the histogram in Fig 4C, introns with splice junction reads and at least 50 exon 2 reads whose gene expression did not change by 2-fold or greater were evaluated.

To call splicing changes using RNA-seq data, we created a control distribution of IAI changes observed in replicate samples where no splicing change should occur, as described above for the array-derived IAIs. In this case the control distribution indicated that an IAI with absolute value >0.3 (or ±25%) could serve as a threshold for splicing change with an FDR of about 0.2.

RT-PCR and qPCR

Relative transcript expression was measured using RT-qPCR of RNA extracted from at least three biological replicates. The graphs shown in Fig 3A and Fig 4B is a measure of expression of a given transcript relative to *SEC65*, a gene whose expression remains constant under all conditions used in this study. For this analysis, two primer pairs were used, one set (within the second exon for intron-containing genes) to measure total RNA for a given gene and one set to measure *SEC65* expression. Relative amount of transcript = $2^{(-\Delta\Delta Ct)}$ where $\Delta\Delta Ct=(Ct_{geneX} - Ct_{SEC65})$.

Splicing efficiency measured by RT-qPCR (such as in Fig 1C and Fig 4D) was calculating using the percent intron-containing transcript from RNA extracted from at least three biological replicates. This analysis employed two primer sets for each gene: one pair for intron-containing pre-mRNA (spanning the 3' splice site), and one set for total RNA (within the second exon). Threshold cycles were determined using reactions containing the same amount of cDNA and the % intron-containing RNA = $2^{(-\Delta\Delta Ct)} * 100$, where $\Delta\Delta Ct=(Ct_{inF\text{-}exR} - Ct_{exF\text{-}exR})_{geneX}$.

Splicing efficiency measured by semi-quantitative RT-PCR (such as in Fig 2B and Fig 3) was determined using the Agilent 2100 Bioanalyzer using RNA extracted from at least three biological replicates. Molar amounts of each PCR product were used to estimate splicing efficiency as follows: %spliced= ((molarity of spliced peak)/(molarity of unspliced peak+ molarity of spliced peak)) *100. Bioanalyzer % spliced values from triplicate biological replicates were averaged and standard deviations are shown.

All RT-PCR and RT-qPCR primers are described in Table S4.

References

Clark, T.A., Sugnet, C.W., and Ares, M., Jr. (2002). Genomewide analysis of mRNA processing in yeast using splicing-specific microarrays. Science *296*, 907-910.
de Hoon, M.J., Imoto, S., Nolan, J., and Miyano, S. (2004). Open source clustering software. Bioinformatics *20*, 1453-1454.
Langmead, B., and Salzberg, S.L. (2012). Fast gapped-read alignment with Bowtie 2. Nat Methods *9*, 357-359.
Munding, E.M., Igel, A.H., Shiue, L., Dorighi, K.M., Trevino, L.R., and Ares, M., Jr. (2010). Integration of a splicing regulatory network within the meiotic gene expression program of Saccharomyces cerevisiae. Genes Dev *24*, 2693-2704.
Saldanha, A.J. (2004). Java Treeview--extensible visualization of microarray data. Bioinformatics *20*, 3246-3248.
Trapnell, C., Pachter, L., and Salzberg, S.L. (2009). TopHat: discovering splice junctions with RNA-Seq. Bioinformatics *25*, 1105-1111.
Yassour, M., Pfiffner, J., Levin, J.Z., Adiconis, X., Gnirke, A., Nusbaum, C., Thompson, D.A., Friedman, N., and Regev, A. (2010). Strand-specific RNA sequencing reveals extensive regulated long antisense transcripts that are conserved across yeast species. Genome Biol *11*, R87.